Journal of Luminescence 166 (2015) 8–16

Contents lists available at ScienceDirect

Journal of Luminescence

journal homepage: www.elsevier.com/locate/jlumin

Study of optical absorption, visible emission and NIR–vis luminescence spectra of Tm^{3+}/Yb^{3+}, Ho^{3+}/Yb^{3+} and $Tm^{3+}/Ho^{3+}/Yb^{3+}$ doped tellurite glasses

M. Seshadri [a,*], L.C. Barbosa [a], C.M.B. Cordeiro [a], M. Radha [a], F.A. Sigoli [b], Y.C. Ratnakaram [c]

[a] Institute of Physics, University of Campinas, UNICAMP, P.O. Box 6165, Campinas 13083-970, Brazil
[b] Institute of Chemistry, University of Campinas, UNICAMP, P.O. Box 6154, Campinas 13083-970, Brazil
[c] Department of Physics, Sri Venkateswara University, SVU, Tirupat 517502, India

ARTICLE INFO

Article history:
Received 10 November 2014
Received in revised form
4 March 2015
Accepted 22 April 2015
Available online 8 May 2015

Keywords:
RE ions
Tellurite glass
Radiative properties
Up-conversion luminescence

ABSTRACT

Tm^{3+}/Yb^{3+}, Ho^{3+}/Yb^{3+} co-doped and $Tm^{3+}/Ho^{3+}/Yb^{3+}$ triply doped TeO_2–Bi_2O_3–ZnO–Li_2O–Nb_2O_5 (TBZLN) tellurite glasses were prepared by melt quenching method. Judd–Ofelt intensity parameters (Ω_λ, $\lambda=2$, 4 and 6), radiative transition probabilities, branching ratios and radiative lifetimes of Tm^{3+}, Ho^{3+} ions in co-doped TBZLN glasses were calculated from the optical absorption spectra. Excitation, visible luminescence and decay lifetimes in visible region were also investigated. The stimulated emission and gain cross-sections for the Tm^{3+}:$^3F_4 \rightarrow {}^3H_6$ (1700 nm) and Ho^{3+}:$^5I_7 \rightarrow {}^5I_8$ (1956 nm) transitions in co-doped TBZLN glasses have been analyzed and compared with those of other reported glasses. Up-conversion luminescence was observed in TBZLN glasses under 980 nm laser excitation and energy transfer mechanisms have been discussed. Finally, CIE color co-ordinates were calculated and it is observed that the color co-ordinates fall in blue and green regions for Tm^{3+}/Yb^{3+} and Ho^{3+}/Yb^{3+} co-doped TBZLN glasses, respectively. A subsequent shift in color co-ordinates from green to greenish-yellow region has been observed with an increase in the concentration (0.1, 0.5 and 1.0 mol%) of Tm^{3+} ions in $Tm^{3+}/Ho^{3+}/Yb^{3+}$ triply doped TBZLN glasses.

1. Introduction

Up-conversion luminescence in rare earths (RE) doped glasses has had an attractive attention since the possibility of development in tunable solid state up-conversion lasers and other photonic applications such as color displays, temperature sensors, etc., [1–5]. It is known that up-conversion luminescence occurs with the availability of at least two low-energy excitation photons (NIR) that are converted into one visible emission photon of higher energy. RE ions such as Er^{3+}, Pr^{3+}, Ho^{3+} and Tm^{3+} are commonly used as activator ions for up-conversion luminescence due to their favorable energy levels. However, these active ions need an effective sensitizer to increase the efficiency of luminescence process with the excitation of commercially available laser diodes (LDs) viz., 980, 808, 785 nm, etc. Among the different sensitizers, Yb^{3+} ion has a relatively high absorption cross-section at 980 nm corresponding to $^2F_{7/2} \rightarrow {}^2F_{5/2}$ transition which facilitate an efficient energy transfer from it to active ions ($Yb^{3+} \rightarrow Pr^{3+}$, Er^{3+}, Ho^{3+}, Tm^{3+}, Tm^{3+}–Ho^{3+}, Tm^{3+}–Er^{3+}).

Currently, there is a strong interest in the development of solid-state laser systems in order to either enhance the efficiencies of the existing devices or to create new ones at visible wavelengths. The efficiencies of various emission levels in the RE doped glasses strongly depend on the host glasses characteristics such as multi-phonon relaxation rate, population of metastable energy levels, energy transfer (ET) and cross-relaxation (CR) rates decided by resonances in the energy level structure and also by the RE ion concentration. Multicomponent oxide glasses are known to be more thermally stable and have better mechanical strength, good chemical durability being superior over the fluoride glasses, and these properties are highly significant for the development of RE doped optical fibers [6]. Among oxide glasses, tellurite glasses possess low phonon energy (750–780 cm^{-1}), excellent transmission in the visible and near infrared up to 4.5 μm, good chemical durability, mechanical stability, good RE ion solubility (10–50 times larger than in silica) and low melting temperature. Moreover, tellurite glasses possess high refractive index that not only facilitates waveguiding but also is useful to increase the spontaneous emission probabilities of radiative

* Corresponding author. Tel.: +55 1935214135; fax: +55 1935215428.
E-mail addresses: seshumeruva@gmail.com, drmeruva@ifi.unicamp.br (M. Seshadri).

http://dx.doi.org/10.1016/j.jlumin.2015.04.022
0022-2313/

transitions in RE ions, making them attractive hosts for up-conversion lasers [7,8].

Normally, the pure TeO_2 glass is unstable because of its lack of linkage between Te–O chains. Some modifier species such as Nb_2O_5, Bi_2O_3, ZnO, PbO, alkali and alkaline earth ions have to be introduced into tellurite glass to improve the linkage between Te–O chains and to connect Te–O chains for stabilizing the glass network. TeO_2–ZnO–R_2O (R=Li, Na, K, Rb, Cs or Ag) glass composition has proven that these glasses have good glass forming tendency with much better resistance to crystallization and susceptibility to moisture than ZBLAN [9]. Also, the relative amount of these constituents allowing various elements thus leads to greater control over variations in performance characteristics. Recently, multicolor emission including white light generation (red, green and blue) has been successfully obtained by infrared to visible up-conversion in tellurite glasses [10–14]. In the present work, the authors reported Tm^{3+}/Yb^{3+} and Ho^{3+}/Yb^{3+} co-doped and $Tm^{3+}/Ho^{3+}/Yb^{3+}$ triply doped TeO_2–Bi_2O_3–ZnO–Li_2O–Nb_2O_3 (TBZLN) tellurite glasses. Spectroscopic studies have been carried out for the co-doped TBZLN glasses. The up-conversion luminescence of prepared glasses has been investigated under 980 nm LD and possible energy transfer mechanisms between sensitizer (Yb^{3+}) and active (Ho^{3+}, Tm^{3+}) ions have been discussed. In addition, multi-color emissions have been described according to the CIE-1931 standards.

2. Experimental

The RE doped TBZLN tellurite glasses investigated in this article were prepared by a melt quenching technique using reagent-grade mixtures of high purity TeO_2 (99.99%), Bi_2O_3 (99.995%), ZnO (99.995%), Li_2CO_3 (99.99%), Nb_2O_5 (99.998%), Tm_2O_3 (99.99%), Ho_2O_3 (99.995%) and Yb_2O_3 (99.99%) compounds. The prepared molar composition of the glasses are as follows:

i. $76.9TeO_2+4.5Bi_2O_3+5.5ZnO+10.5Li_2O+1.5Nb_2O_5+0.1Tm_2O_3+1.0Yb_2O_3$;
ii. $76.5TeO_2+4.5Bi_2O_3+5.5ZnO+10.5Li_2O+1.5Nb_2O_5+0.5Ho_2O_3+1.0Yb_2O_3$ and
iii. $(76.5-x)TeO_2+4.5Bi_2O_3+5.5ZnO+10.5Li_2O+1.5Nb_2O_5+xTm_2O_3+0.5Ho_2O_3+1.0Yb_2O_3$ (x=0.1, 0.5, 1.0 and 1.5 mol%).

About 20 g glass batches were melted in the radio frequency induction furnace (5 MHz) at temperature between 850 and 950 °C for 1–3 h in a platinum crucible covered with silica plate. The melts were cooled into a preheated brass plate and moved into another oven to anneal the glasses at glass transition temperature for 2 h to remove the internal stress. Then the samples were polished for optical measurements.

The absorption spectrum was recorded with a Varian Cary 5000 UV–vis–NIR spectrophotometer in the wavelength range 400–2200 nm. The visible luminescence and decay measurements were carried out using Jobin Yvon Fluorolog-3 spectrofluorimeter (Horiba FL3-22iHR320) with 450 W Xenon arc and 150 W Xenon flash lamps as pump sources. The NIR to vis up-conversion emission spectra were measured using a 980 nm crystal laser (DL series). All the measurements were carried out at room temperature.

Table 1 shows the physical and optical properties for Tm^{3+}/Yb^{3+} and Ho^{3+}/Yb^{3+} co-doped TBZLN glasses. The densities of the glass samples were determined according to the Archimedes principle using distilled water as an immersion liquid. Refractive index was measured by a prism coupling method (Metricon Model 2010) at 633 nm.

Table 1
Certain physical properties of Tm^{3+} and Ho^{3+} ions in co-doped TBZLN glasses.

Parameter	Tm^{3+}/Yb^{3+}	Ho^{3+}/Yb^{3+}
Average molecular weight, M (g)	164.2	165.1
Density, d (g/cm^3)	4.212	4.142
Refractive index, n_d (633 nm)	2.104	2.104
Molar refractivity, R_M (cm^{-3})	20.762	21.222
Dielectric constant, ε	4.415	4.415
Polarisability, $\alpha_e \times 10^{24}$ (cm^3)	8.231	8.414
Ion concentration, $N \times 10^{20}$ (ions/cm^3)	0.309	1.509
Ionic radius, r_i (Å)	12.841	7.578
Inter ionic distance, r_p (Å)	31.869	18.782
Field strength, $F \times 10^{-14}$ (cm^2)	1.819	5.238
Reflection loss, R%	12.611	12.611
Optical energy band gap, E_{opt} (eV)	2.853	3.016

3. Results and discussion

3.1. Absorption spectra and Judd–Ofelt analysis

Fig. 1(a) shows the optical absorption spectra of Tm^{3+}/Yb^{3+}, Ho^{3+}/Yb^{3+} and $Tm^{3+}/Ho^{3+}/Yb^{3+}$ doped TBZLN glasses in the vis/NIR region (400–2200 nm). The observed absorption bands attributed to the intra-configurational f–f electronic transitions from the ground state to excited states of RE ions. The absorption band assignments are shown in Fig. 1(a) for the respective RE ions. The absorption edge of amorphous materials gives a measurement of the band strength or energy gap. McSwin et al. [15] suggested that the shift of absorption band edges in amorphous materials can be related to the non-bridging oxygen (NBO) which binds electrons less tightly than bridging oxygen (BO). It is known that optical absorption edge in amorphous materials at absorption coefficients $>10^4$ cm^{-1} is interpreted in terms of indirect transitions across an optical band gap. Optical band gap values were obtained for indirect transitions of Tm^{3+}/Yb^{3+} and Ho^{3+}/Yb^{3+} co-doped TBZLN glasses from the variation of $(\alpha\hbar\omega)^{1/2}$ with $\hbar\omega$ graphs (see Fig. 1(b)) using Davis and Mott theory as explained in our earlier articles [16,17]. The respective values of E_{opt} are obtained by extrapolating to $(\alpha\hbar\omega)^{1/2}=0$ for indirect transitions. It is observed that 2.85 eV and 3.01 eV are the energy band gaps for the Tm^{3+}/Yb^{3+} and Ho^{3+}/Yb^{3+} co-doped TBZLN glasses, respectively, and are in good agreement with other reported tellurite glasses [18,19].

The experimental (f_{exp}) and calculated (f_{cal}) oscillator strengths were determined for Tm^{3+} and Ho^{3+} ions in Tm^{3+}/Yb^{3+}, Ho^{3+}/Yb^{3+}co-doped TBZLN glasses using the expressions given in Ref. [20] considering only Tm^{3+}, Ho^{3+} absorption peaks and eliminating the Yb^{3+} absorption peak in both the spectra respectively and are presented in Table 2 along with root mean square (rms) deviations. The hypersensitive transitions (HSTs), Tm^{3+}:$^3H_6 \rightarrow {}^3F_4$, $^3H_6 \rightarrow {}^3H_4$ and $^3H_6 \rightarrow {}^1G_4$ [21] and Ho^{3+}:$^5I_8 \rightarrow {}^5G_6$ [20] are intense and have large magnitude of oscillator strength of the transitions depending strongly on neighboring ligands of RE ions. These transitions obey the selection rule, $\Delta J \leq 2$, $\Delta L \leq 2$ and $\Delta S=0$ and exhibit high values of $\|U^{(2)}\|^2$ doubly reduced matrix elements. In the case of Tm^{3+}/Yb^{3+}, Ho^{3+}/Yb^{3+}co-doped TBZLN glasses, the observed oscillator strength (f_{exp}) ($\times 10^{-6}$) of HSTs, Tm^{3+}:$^3H_6 \rightarrow {}^3F_4$ (7.29), $^3H_6 \rightarrow {}^1G_4$ (5.05) are higher than Ba–La tellurite [22] and LKBBT tellurite [23] glasses; and Ho^{3+}:$^5I_8 \rightarrow {}^5G_6$ (39.62) is higher than those of SANZ [23] and is similar to borophosphate (LBMBPH4) [24] glasses. The higher magnitude of oscillator strengths of the HSTs indicates a higher crystal field asymmetry of Tm^{3+} and Ho^{3+} chemical environments in co-doped TBZLN glasses [21]. From Table 2, it is observed that the low root mean square (rms) deviation between the experimental and calculated oscillator strengths indicates the validity of Judd–Ofelt theory [25,26].

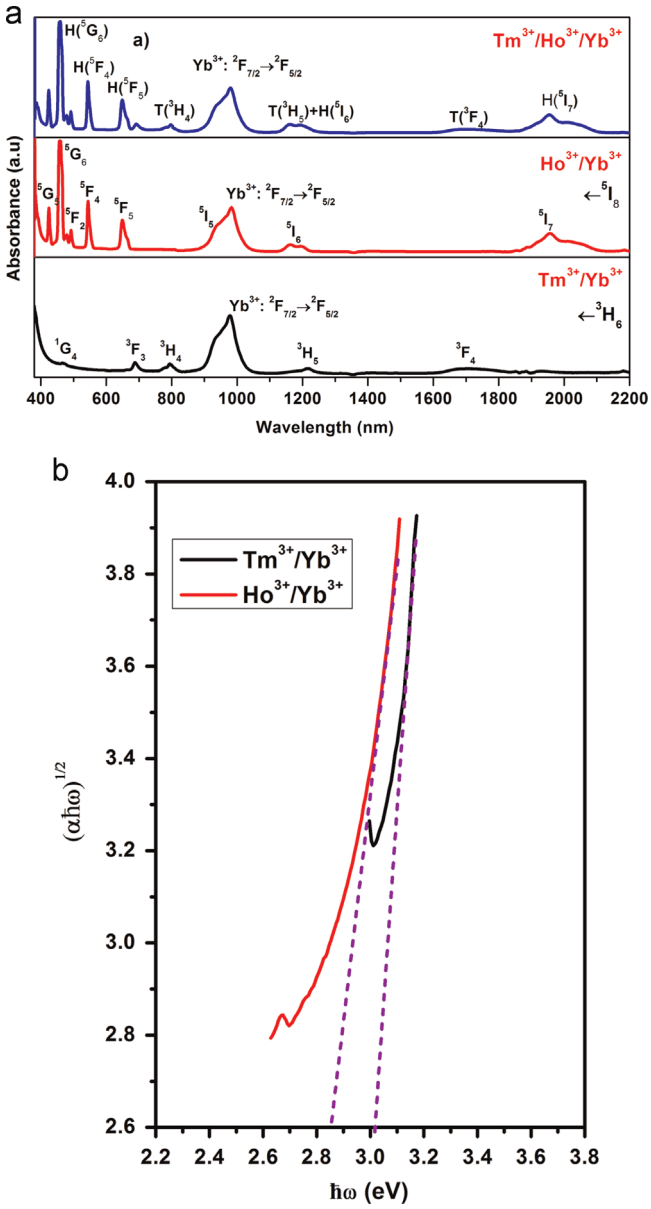

Fig. 1. (a) Optical absorption spectra of $0.1Tm^{3+}/1.0Yb^{3+}$, $0.5Ho^{3+}/1.0Yb^{3+}$ co-doped and. $0.1Tm^{3+}/0.5Ho^{3+}/1.0Yb^{3+}$ triply doped TBZLN glasses. (b) Relation between $(\alpha\hbar\omega)^{1/2}$ and $(\hbar\omega)$ for co-doped TBZLN glasses.

Using the experimental oscillator strengths, a best set of J–O intensity parameters Ω_λ (λ=2, 4 and 6) for the Tm^{3+} and Ho^{3+} ions in co-doped glass matrices were determined using the procedure followed in Ref. [21] and are presented in Table 3 along with some data of other host glasses. These J–O intensity parameters depend on the host glass composition. It is known that Ω_2 is related to asymmetry of the electric field around the RE ions whereas Ω_4 and Ω_6 are related to the rigidity of the host glass matrix. The sum of the three J–O intensity parameters ($\Sigma\Omega_\lambda$) can also be related to the covalency degree of RE–O bond [27]. It is found from Table 3 that Ω_2 (or $\Sigma\Omega_\lambda$) values for Tm^{3+} and Ho^{3+} ions in co-doped TBZLN glasses are higher than those reported tellurite [22,28,29,32,34] and other host glasses [24,30–33,35,36] indicating that a strong asymmetry and certain covalency degree persists between the RE^{3+} ions and ligands. The order of magnitude of J–O intensity parameters $\Omega_2 > \Omega_6 > \Omega_4$ for Tm^{3+}/Yb^{3+} co-doped TBZLN glass follows the trend of Bi-silicate [30] and K–Mg–Al phosphate [31] glasses and for Ho^{3+}/Yb^{3+} co-doped TBZLN glass, $\Omega_2 > \Omega_4 > \Omega_6$ is comparable with the other glasses [24,33–36].

Table 2
Experimental energies (ν) (cm^{-1}), oscillator strengths (f) ($\times 10^{-6}$) of Tm^{3+}, Ho^{3+} ions in co-doped TBZLN glasses.

Transitions	ν	f_{exp}	f_{cal}
Tm^{3+}			
$^1G_4$	21459	4.39	2.09
$^3F_2$, $^3F_3$	14535	12.20	12.58
$^3H_4$	12594	13.01	12.78
$^3H_5$	8224	7.35	6.92
$^3F_4$	5882	6.94	6.98
δ_{rms}	$\pm$0.43		
Ho^{3+}			
$^5I_7$	5107	3.54	3.43
$^5I_6$	8621	1.86	2.48
$^5F_5$	15504	8.01	7.70
$^5S_2(^5F_4)$	18519	9.94	9.38
$^5F_3$	20492	2.57	2.62
$^5F_2$	21053	0.61	1.49
$^3K_8$	21277	0.31	2.06
$^5G_6$	22124	39.60	39.79
$^5G_5$	23810	7.90	8.56
δ_{rms}	$\pm$0.93		

Table 3
J–O parameters (Ω_λ, λ=2, 4 and 6) ($\times 10^{-20}$) (cm^2) of Tm^{3+} and Ho^{3+} ions in TBZLN glasses long with various host glasses.

Glass	Ω_2	Ω_4	Ω_6	$\Sigma\Omega_\lambda$	Trend
Tm^{3+}					
TBZLN[a]	9.44	0.22	5.58	15.24	$\Omega_2 > \Omega_6 > \Omega_4$
Barium-tellurite [28]	5.32	2.55	1.12	8.87	$\Omega_2 > \Omega_4 > \Omega_6$
Ba–La-tellurite [22]	7.15	3.33	1.28	11.76	$\Omega_2 > \Omega_4 > \Omega_6$
TPBL [29]	4.72	1.35	1.21	7.28	$\Omega_2 > \Omega_4 > \Omega_6$
Bi-silicate [30]	3.17	0.36	0.54	4.07	$\Omega_2 > \Omega_6 > \Omega_4$
Phosphate [31]	9.32	1.82	3.21	14.35	$\Omega_2 > \Omega_4 > \Omega_6$
Fluoride [32]	2.27	1.16	0.11	3.54	$\Omega_2 > \Omega_6 > \Omega_4$
TZN [32]	5.10	1.17	1.08	7.35	$\Omega_2 > \Omega_4 > \Omega_6$
Ho^{3+}					
TBZLN[a]	5.59	4.85	2.66	13.10	$\Omega_2 > \Omega_4 > \Omega_6$
Borophosphate [24]	4.32	2.55	1.70	8.57	$\Omega_2 > \Omega_4 > \Omega_6$
Oxyfluoride [33]	4.20	2.80	1.10	8.57	$\Omega_2 > \Omega_4 > \Omega_6$
Germanotellurite [34]	4.25	2.48	1.31	8.04	$\Omega_2 > \Omega_4 > \Omega_6$
Fluorophosphate [35]	2.50	3.09	1.31	6.90	$\Omega_2 > \Omega_4 > \Omega_6$
$Na_4AlZnP_3O_{12}$ glass [36]	4.65	2.02	1.34	8.01	$\Omega_2 > \Omega_4 > \Omega_6$

[a] Present work.

Using J–O intensity parameters (Ω_λ), spontaneous transition probabilities (A_{rad}), total radiative transition probabilities (ΣA_{rad}), branching ratios (β) and radiative lifetimes (τ_{rad}) were estimated for certain excited levels of RE doped glasses [20]. The total radiative transition probabilities A_R, τ_R and β of certain emission transition of Tm^{3+} and Ho^{3+} ions in co-doped TBZLN glasses are presented in Table 4. From the observed energy separation between $^3F_2$ and $^3F_3$ levels (559 cm^{-1}) of Tm^{3+} ions, and separation between $^5F_4$ and $^5S_2$ levels (97 cm^{-1}) of Ho^{3+} ions, thermalization may occur for the two levels (Ho^{3+}:$^5F_4$, $^5S_2$; Tm^{3+}:$^3F_2$ and $^3F_3$) in co-doped tellurite glasses. It is known that the efficiency of fluorescence levels is related to the non-radiative relaxation rates from excited states. According to the theory for non-radiative relaxations rates in glasses, the multiphonon relaxation rates between two adjacent levels of Tm^{3+} and Ho^{3+} ions in co-doped TBZLN glasses are estimated using the expression described elsewhere [37]. Table 4 describes the multiphonon relaxation rates (W_{NR}) for various excited states of Tm^{3+} and Ho^{3+} ions in TBZLN glasses. It is observed that among the various excited states of Tm^{3+} and Ho^{3+} ions, the levels $^3F_2$ (Tm^{3+}) and $^3F_3$ (Tm^{3+})

Table 4
Certain radiative and non-radiative properties of Tm^{3+}, Ho^{3+} ions in co-doped TBZLN glasses.

Transitions	A_T (s^{-1})	τ_R (μs)	β (%)	W_{NR} (s^{-1})
Tm^{3+}				
$^1D_2 \rightarrow {}^3H_6$	65310.2	15.3	13.8	6.39E−45
$^1G_4 \rightarrow {}^3H_6$	14166.3	70.6	29.1	8.96E−32
$^3F_2 \rightarrow {}^3H_6$	11721.1	85.3	59.6	6.19E−19
$^3F_3 \rightarrow {}^3H_6$	16661.5	60.0	87.1	8.25E−18
$^3H_4 \rightarrow {}^3H_6$	8982.2	111.3	93.5	6.58E−14
$^3H_5 \rightarrow {}^3H_6$	1675.0	597.0	97.0	3.56E−05
$^3F_4 \rightarrow {}^3H_6$	1052.7	949.9	100.0	1.53E+00
Ho^{3+}				
$^5F_4 \rightarrow {}^5I_8$	19328.3	51.7	78.8	4.94E−26
$^5F_5 \rightarrow {}^5I_8$	10884.3	91.9	77.3	9.26E−20
$^5I_4 \rightarrow {}^5I_8$	221.5	4514.7	13.2	3.63E−13
$^5I_5 \rightarrow {}^5I_8$	653.4	1573.8	41.1	4.88E−11
$^5I_6 \rightarrow {}^5I_8$	786.8	1270.9	90.3	5.77E−06
$^5I_7 \rightarrow {}^5I_8$	300.0	3333.3	100.0	4.97E+01

and $^5F_4$ (Ho^{3+}) show lower non-radiative relaxation rates than the $^3F_4$ (Tm^{3+}) and $^5I_7$ (Ho^{3+}) levels.

3.2. Visible luminescence and McCumbers analysis

Fig. 2(a) and (b) shows visible luminescence spectra of Tm^{3+}/Yb^{3+} and Ho^{3+}/Yb^{3+} co-doped TBZLN glasses. The insets of Fig. 2(a) and (b) show the excitation spectra of Tm^{3+}/Yb^{3+} and Ho^{3+}/Yb^{3+} co-doped TBZLN glasses measured at room temperature by monitoring the wavelengths 454 and 546 nm, respectively. The excitation band at 352 nm in the Tm^{3+}/Yb^{3+} co-doped TBZLN glass is attributed to $^1D_2 \rightarrow {}^3H_6$ transition of Tm^{3+} ions whereas the excitation bands at 360, 385, 417, 450, 467 and 485 nm in the Ho^{3+}/Yb^{3+} co-doped TBZLN glass are attributed to $^3H_5(^3H_6) \rightarrow {}^5I_8$, $^5G_4(^3K_7) \rightarrow {}^5I_8$, $^5G_5 \rightarrow {}^5I_8$, $^5G_6 \rightarrow {}^5I_8$, $^3K_8(^5F_2) \rightarrow {}^5I_8$ and $^5F_3 \rightarrow {}^5I_8$ transitions of Ho^{3+} ions. Under 352 nm excitation, the 454, 480 and 710 nm emission bands are observed in Tm^{3+}/Yb^{3+} co-doped TBZLN glasses which are attributed to the $^1D_2 \rightarrow {}^3H_4$, $^1G_4 \rightarrow {}^3H_6$ and $^3F_3 \rightarrow {}^3H_6$ transitions of Tm^{3+} ions, respectively. Under 450 nm excitation, the 546 and 660 nm emission bands attributed to $^5F_4(^5S_2) \rightarrow {}^5I_8$ and $^5F_5 \rightarrow {}^5I_8$ transitions of Ho^{3+} in Ho^{3+}/Yb^{3+} co-doped TBZLN glass are found. The stimulated emission cross-section (σ_{emi}) gives information about the potential laser transitions of RE ions in any host matrix and its value signifies the rate of energy extracted from the lasing material. J–O theory successfully account for the induced emission cross-section. The peak stimulated emission cross-section, $\sigma_P(\lambda)$ is calculated using the procedure followed by elsewhere [19]. Since the emission band has asymmetry, the area under each emission peak is used instead of full-width at half-maximum (FWHM) in the calculations. The effective line width is defined as $\Delta\lambda_{eff} = \frac{\int I(\lambda)d\lambda}{I_{max}}$, I_{max} is the maximum intensity at fluorescence emission peaks. In the present work, emission band positions (λ_P), effective line widths ($\Delta\lambda_{eff}$), radiative transition probabilities (A_{rad}) and stimulated emission cross-sections (σ_P) of emission transitions for Tm^{3+} and Ho^{3+} ions in co-doped TBZLN glasses are determined and presented in Table 5. The peak stimulated emission cross-sections for the useful stimulated emission transitions of Tm^{3+} and Ho^{3+} ions in Tm^{3+}/Yb^{3+} and Ho^{3+}/Yb^{3+} co-doped TBZLN glasses are also estimated from their corresponding ground state absorption cross-section $\sigma_a(\lambda)$ using McCumber's theory as explained in our previous paper [16]. The absorption and emission cross-sections (from McCumber's theory) spectra of Tm^{3+}/Yb^{3+} and Ho^{3+}/Yb^{3+} co-doped TBZLN glasses are shown in Fig. 3 along with the absorption cross-section of Yb^{3+} ($^2F_{7/2} \rightarrow {}^2F_{5/2}$). The estimated emission cross-sections for the Tm^{3+}:$^3F_4 \rightarrow {}^3H_6$ and Ho^{3+}:$^5I_7 \rightarrow {}^5I_8$ transitions in Tm^{3+}/Yb^{3+} and Ho^{3+}/Yb^{3+} co-doped TBZLN glasses are listed in Table 5. The large

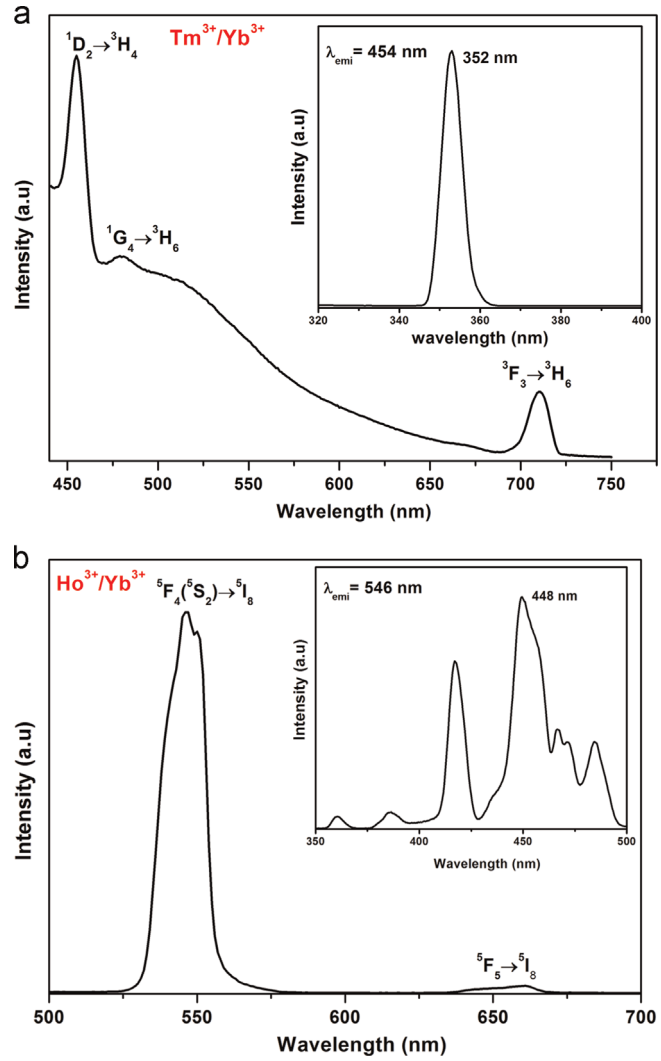

Fig. 2. (a) Visible luminescence spectra of Tm^{3+}/Yb^{3+} co-doped TBZLN glass (λ_{exc}=0.352 nm). Inset shows the excitation spectrum of Tm^{3+}/Yb^{3+} co-doped TBZLN glass (λ_{exc}=454 nm). (b) Visible luminescence spectra of Ho^{3+}/Yb^{3+} co-doped TBZLN glass (λ_{exc}=0.448 nm). Inset shows the excitation spectrum of Ho^{3+}/Yb^{3+} co-doped tellurite glass (λ_{exc}=546 nm).

Table 5
Peak wavelength (λ_P) (nm), effective linewidths ($\Delta\lambda_{eff}$) (nm), radiative transition probabilities (A_{rad}) (s^{-1}) and stimulated emission cross-sections (σ_{emi}) ($\times 10^{-20}$ cm^2) of Tm^{3+} and Ho^{3+} ions in co-doped TBZLN glasses.

Transitions	λ_P	$\Delta\lambda_{eff}$	A_{rad}	σ_{emi}
Tm^{3+}				
$^1D_2 \rightarrow {}^3F_4$	454	11	45321	5.48
$^1G_4 \rightarrow {}^3H_6$	480	15	4118.8	0.42
$^3F_3 \rightarrow {}^3H_6$	711	14	14517.2	8.13
$^3F_4 \rightarrow {}^3H_6$	1702	–	1052.7	1.25[a]
Ho^{3+}				
$^5F_4(^5S_2) \rightarrow {}^5I_8$	545	16	15234.8	2.50
$^5F_5 \rightarrow {}^5I_8$	660	19	8408.2	2.49
$^5I_7 \rightarrow {}^5I_8$	1952	–	300.0	0.93[a]

[a] From McCumber's theory.

stimulated emission cross-sections are attractive features for low threshold, high gain applications and are utilized to obtain CW laser.

From Table 5, it is observed that among the three visible emission transitions of Tm^{3+} ions, the $^1D_2 \rightarrow {}^3F_4$ (454 nm) transition shows higher emission cross-section and is higher than the K–Mg–Al phosphate [31] glass (4.59×10^{-20} cm^2). For Ho^{3+} ions in co-doped tellurite glass, the

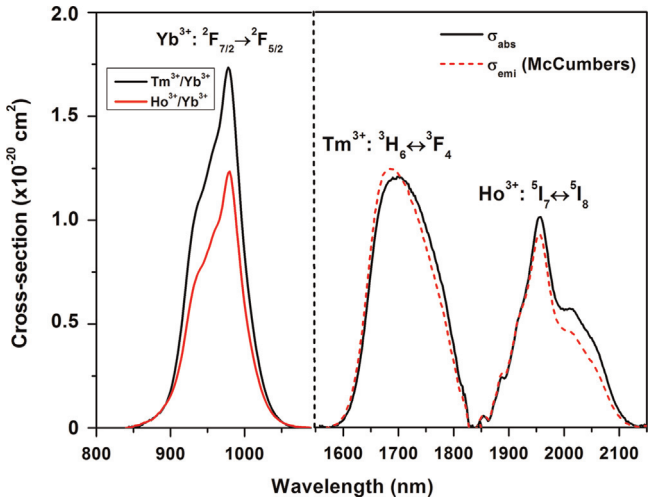

Fig. 3. Absorption and emission cross-sections of Tm^{3+}:$^3F_4 \rightarrow {}^3H_6$ and Ho^{3+}:$^5I_7 \rightarrow {}^5I_8$. transitions for co-doped TBZLN glasses along with absorption cross-section of Yb^{3+} ($^2F_{7/2} \rightarrow {}^2F_{5/2}$).

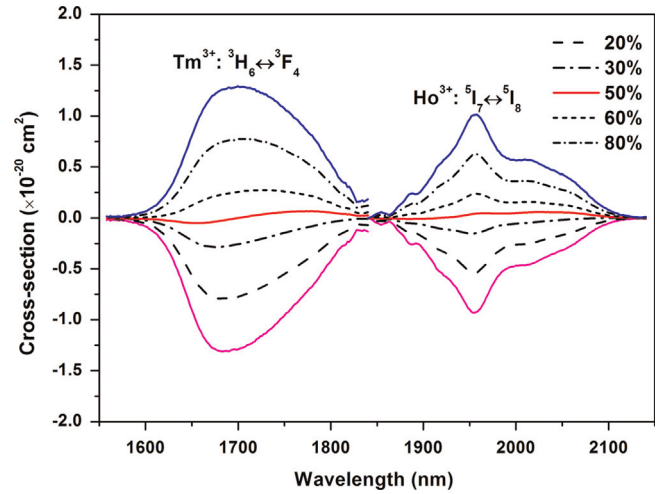

Fig. 4. Gain cross-section of Tm^{3+}:$^3F_4 \rightarrow {}^3H_6$ and Ho^{3+}:$^5I_7 \rightarrow {}^5I_8$ transitions for co-doped TBZLN glasses.

$^5F_4(^5S_2) \rightarrow {}^5I_8$ (546 nm) and $^5F_5 \rightarrow {}^5I_8$ (660 nm) transitions have similar magnitude of emission cross-sections and the transition $^5F_4(^5S_2) \rightarrow {}^5I_8$ is quite useful laser transition in designing of green emitting lasers due to its higher branching ratio compared to other transitions. The magnitude of emission cross-section of the $^5F_4(^5S_2) \rightarrow {}^5I_8$ transition of Ho^{3+} ions in Ho^{3+}/Yb^{3+} co-doped TBZLN glass is higher than the values of P_2O_5–K_2O–Al_2O_3–PbO–Na_2O (1.43×10^{-20} cm^2) [38], TeO_2–ZnO–PbO–PbF_2–Na_2O (0.8×10^{-20} cm^2) [18] and PbO–Al_2O_3–B_2O_3 (0.42×10^{-20} cm^2) [39] glasses. The magnitude of stimulated emission cross-section of Tm^{3+}:$^3F_4 \rightarrow {}^3H_6$ transition (1.25×10^{-20} cm^2) in Tm^{3+}/Yb^{3+} co-doped TBZLN glass is higher than those reported for silicate (0.362×10^{-20} cm^2) [40], germinate (0.488×10–^{20} cm^2) [41] and Bi_2O_3–GeO_2–Na_2O (0.62×10^{-20} cm^2) [42] glass hosts. For Ho^{3+}:$^5I_7 \rightarrow {}^5I_8$ transition, the magnitude of stimulated emission cross-section (0.93×10^{-20} cm^2) in Ho^{3+}/Yb^{3+} co-dope TBZLN glass is higher than those reported for silicate (0.307×10^{-20} cm^2) [43], germinate (0.469×10^{-20} cm^2) [41], and Bi_2O_3–GeO_2–ZnO (0.533×10^{-20} cm^2) [44] glass hosts. The high magnitude of stimulated emission cross-sections in co-doped TBZLN glasses is due to the high spontaneous radiative transition probabilities resulting from the high refractive index of the TBZLN glasses (2.104). The gain value of laser material is very important and is estimated by the product of stimulated emission cross-section (σ_{emi}) and radiative lifetime (τ_R) of fluorescent levels. It is observed that the $\sigma_{emi} \times \tau_R$ is 11.87×10^{-24} cm^2 s and 30.99×10^{-24} cm^2 s for the Tm^{3+}:$^3F_4 \rightarrow {}^3H_6$ and Ho^{3+}:$^5I_7 \rightarrow {}^5I_8$ transitions in co-doped TBZLN glasses, respectively.

In addition, we have calculated the optical gain cross-section $G(\lambda)$ which is related with absorption and emission cross-sections through the population inversion parameter (γ) and can be expressed as [20]

$$G(\lambda) = \gamma\sigma_{emi}(\lambda) - (1-\gamma)\sigma_{abs}(\lambda) \quad (1)$$

Fig. 4 represents the grain cross-section for the Tm^{3+}:$^3F_4 \rightarrow {}^3H_6$ and Ho^{3+}:$^5I_7 \rightarrow {}^5I_8$ transitions in co-doped TBZLN glasses. It is observed that a positive value of gain cross-section at 50% of population inversion factor covers broad wavelength ranges of 1702–1820 nm and 1917–2100 nm for Tm^{3+}/Yb^{3+} and Ho^{3+}/Yb^{3+} co-doped TBZLN glasses, respectively.

The fluorescence decay curves of the $^1D_2$ (Tm^{3+}), $^5F_4(^5S_2)$ (Ho^{3+}) and $^5F_5$ (Ho^{3+}) levels were measured at 454, 545 and 660 nm for the Tm^{3+}/Yb^{3+} and Ho^{3+}/Yb^{3+} co-doped TBZLN glasses (Fig. 5). The experimental lifetimes were determined by taking the first e-folding times of the decay curves and are 13.2, 24.8, 25.8 μs for the $^1D_2$ (Tm^{3+}), $^5F_4(^5S_2)$ (Ho^{3+}) and $^5F_5$ (Ho^{3+}) levels, respectively. One can easily estimate the quantum efficiency (QE) of the fluorescence level with the known values of measured lifetimes and known values of theoretical lifetimes (from J–O theory) by using the expression, $\eta = \tau_{exp}/\tau_{cal}$. The QE for $^1D_2$ (Tm^{3+}) level in Tm^{3+}/Yb^{3+} co-doped TBZLN glass is 86% and is comparable to the QE values of 0.1 mol% Tm^{3+} doped calcium fluoroborate glass [45] and K–Mg–Al phosphate glass [31], respectively. For $^5F_4(^5S_2)$, $^5I_8$ and $^5F_5$ levels of Ho^{3+} ions in Ho^{3+}/Yb^{3+} co-doped TBZLN glass, the QE values are 48% and 28%, respectively.

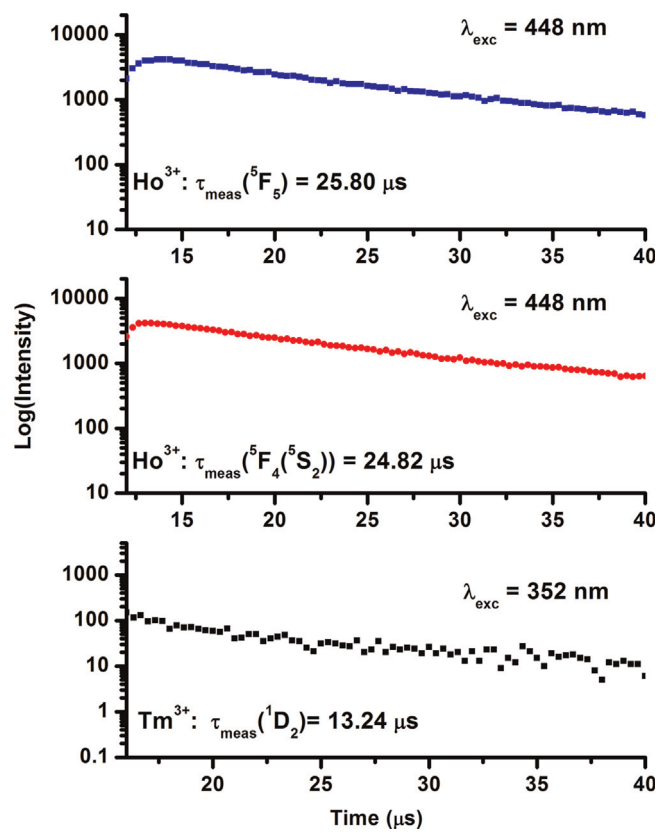

Fig. 5. Decay profiles of $^1D_2$ (Tm^{3+}) (λ_{exc}=352 nm), $^5F_4(^5S_2)$ and $^5F_5$ (Ho^{3+}) (λ_{exc}=448 nm) in co-doped TBZLN glasses.

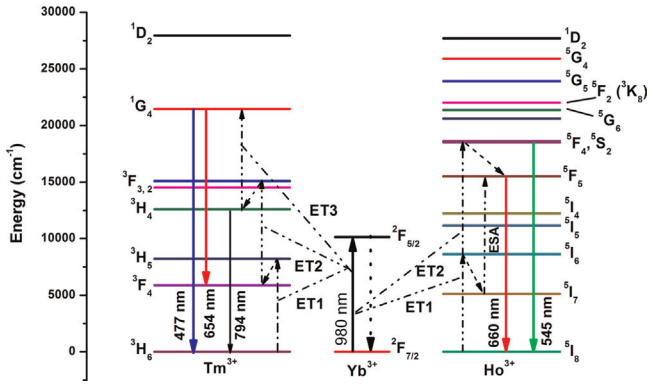

Fig. 6. Schematic energy level diagram of Tm^{3+}, Ho^{3+} and Yb^{3+} ions and possible energy. transfer process in co-doped and triply doped TBZLN glasses.

3.3. Up-conversion luminescence

As shown in Fig. 3, the large absorption of Yb^{3+}:$^2F_{7/2}\rightarrow{}^2F_{5/2}$ transition is beneficial for obtaining enough pumping energy and transferring considerable energy to Tm^{3+} or Ho^{3+} ions in co-doped TBZLN glasses. Generally, the up-conversion energy transfer is quite effective due to the proper energy matching and favourable metastable states. Fig. 6 shows the schematic diagram of up-conversion process and energy level structure of RE^{3+} ions. In the present work, the up-conversion luminescence of Tm^{3+}/Yb^{3+} and Ho^{3+}/Yb^{3+} doped TBZLN glasses was measured under 980 nm excitation. It is well known that the up-converted emission intensity I_{up} is proportional to mth power of IR excitation intensity I_{IR}, i.e. $I_{up}\alpha I_{IR}^{m}$, where m is the number of IR photons involved in the process. The dependence of up-conversion luminescence intensities for different pump powers was analyzed and is illustrated in a plot of logarithmic emission intensities as a function of logarithmic pump power of laser yielding a straight line with slope m for the observed emission bands. The possible infrared to visible luminescence mechanism leading to the population of excited levels of RE (Ho^{3+}, Tm^{3+}) ions in the presence of Yb^{3+} ions as sensitizers under excitation at 980 nm excitation has been explained as follows.

3.3.1. Blue emission in Tm^{3+}/Yb^{3+} co-doped TBZLN glass

Fig. 7(a) shows the observed up-conversion luminescence in Tm^{3+}/Yb^{3+} co-doped TBZLN glass as a function of pump power laser. The emission bands at 480, 652 and 793 nm are attributed to the $^1G_4\rightarrow{}^3H_6$, $^1G_4\rightarrow{}^3F_4$ and $^3H_4\rightarrow{}^3H_6$ transitions of Tm^{3+} ions, respectively. It is observed that the $^3H_4\rightarrow{}^3H_6$ transition is more intense than the $^1G_4\rightarrow{}^3H_6$, $^1G_4\rightarrow{}^3F_4$ transitions. Among the visible transitions, $^1G_4\rightarrow{}^3H_6$ is more intense and it needs to require a three photon absorption either from Tm^{3+} ions or phonon assisted energy transfer from Yb^{3+} to Tm^{3+} ions. As shown in Fig. 7(b), the fitted slopes found for the two visible up-conversion transitions at 480, 652 and for NIR emission transition at 793 nm are 2.96, 1.97 and 2.08, respectively, indicating that blue shows cubic and red and NIR emissions shows approximately quadratic dependence on the excitation power. Hence the blue emission is populated by the three photon process whereas red and NIR emissions is originated from the two photon process.

According to the energy matching conditions (see Fig. 6), 980 nm laser diode used as pumping source for the Tm^{3+}/Yb^{3+} co-doped TBZLN glass, Tm^{3+} cannot absorb 980 nm photons due to lack of matched energy level whereas Yb^{3+} ions can absorb the near infrared radiation efficiently and transfer their excitation energy to Tm^{3+} ions. The Tm^{3+} ions can populate the $^1G_4$ levels through the following energy transfer steps:

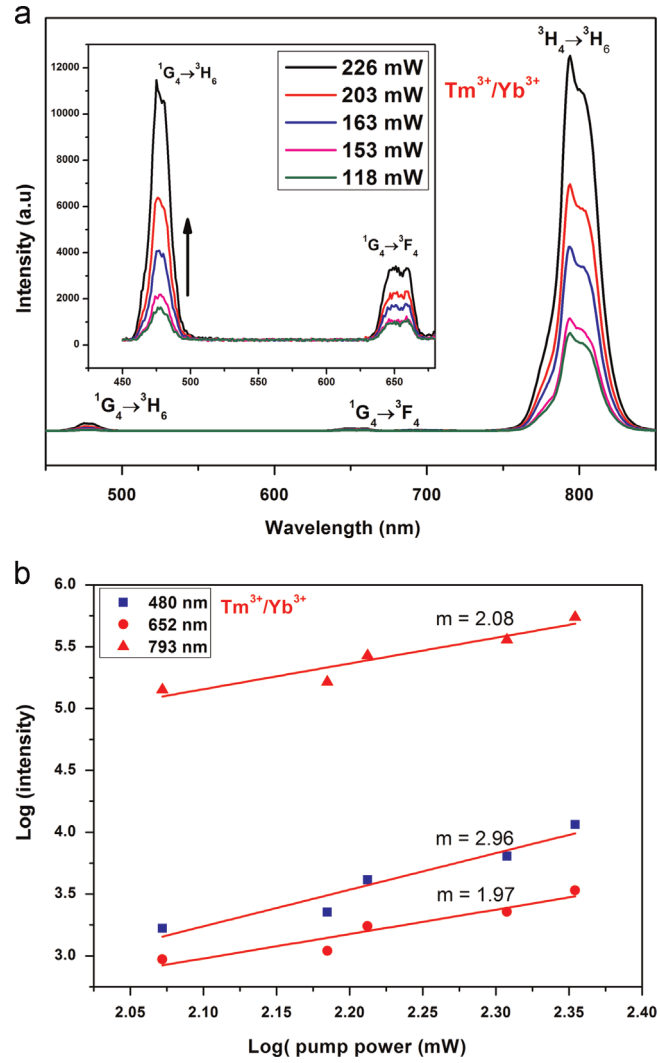

Fig. 7. Up-conversion luminescence spectra of Tm^{3+}/Yb^{3+} co-doped TBZLN glass as a function of pump power (λ_{exc}=980 nm). Inset shows logarithmic pump power vs intensity of blue and red emissions.

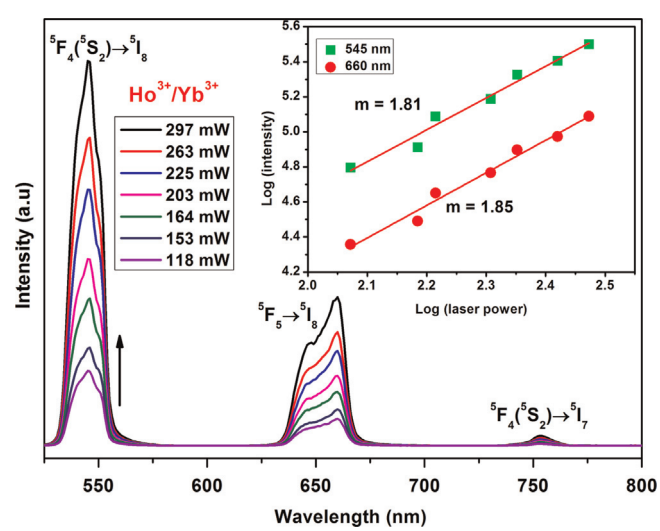

Fig. 8. Up-conversion luminescence spectra of Ho^{3+}/Yb^{3+} co-doped TBZLN glass as a function of pump power (λ_{exc}=980 nm). Inset shows logarithmic pump power vs intensity of green and red emissions.

(i) Some part of energy may be transferred from first excited Yb^{3+} ions to Tm^{3+} ions, thus the $^3H_5$ level is populated through the first energy transfer process:

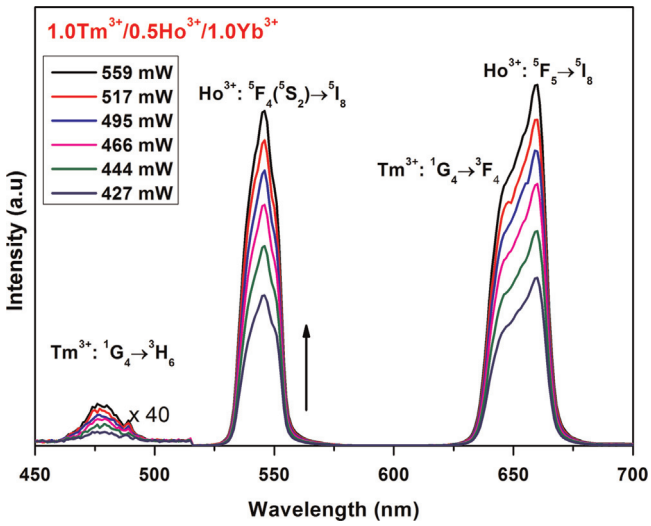

Fig. 9. Up-conversion luminescence spectra of $Tm^{3+}/Ho^{3+}/Yb^{3+}$ co-doped TBZLN glass as a function of pump power (λ_{exc}=980 nm).

ET1: $^2F_{5/2}$ $(Yb^{3+})+{}^3H_6(Tm^{3+})\rightarrow{}^2F_{7/2}$ $(Yb^{3+})+{}^3H_5(Tm^{3+})$

(ii) Then the $^3H_5$ level non-radiatively relax to $^3F_4$ level and excites the $^3F_2$, $^3F_3$ levels by the second excited Yb^{3+} ions. Thus the energy transfer process is:

ET2: $^2F_{5/2}$ $(Yb^{3+})+{}^3F_4(Tm^{3+})\rightarrow{}^2F_{7/2}$ $(Yb^{3+})+{}^3F_{2,3}(Tm^{3+})$

As the case above, energy transfer from Yb^{3+} to Tm^{3+} ions is considered to be efficient, and the relaxation process of $^3F_{2,3}$ (Tm^{3+}) to $^3H_4$ (Tm^{3+}) will be effective due to narrow energy gap between them (2501 cm^{-1}).

(iii) The population of $^1G_4$ level from the $^3H_4$ level of Tm^{3+} ions by the third excited Yb^{3+} ions to Tm^{3+} ions. Thus the third energy transfers process is:

ET3: $^2F_{5/2}$ $(Yb^{3+})+{}^3H_4$ $(Tm^{3+})\rightarrow{}^2F_{7/2}$ $(Yb^{3+})+{}^1G_4$ (Tm^{3+})

Finally, $^1G_4$ level radiatively relaxes to $^3H_6$ and $^3F_4$ levels corresponding to the 478 (blue) and 650 nm (red) emission bands. For NIR emission, $^3F_2$, $^3F_3$ levels relax to $^3H_4$ level and then radiatively relax to $^3H_6$ level correspond to strong emission band at 793 nm ($^3H_4\rightarrow{}^3H_6$) (see Fig. 7(a)).

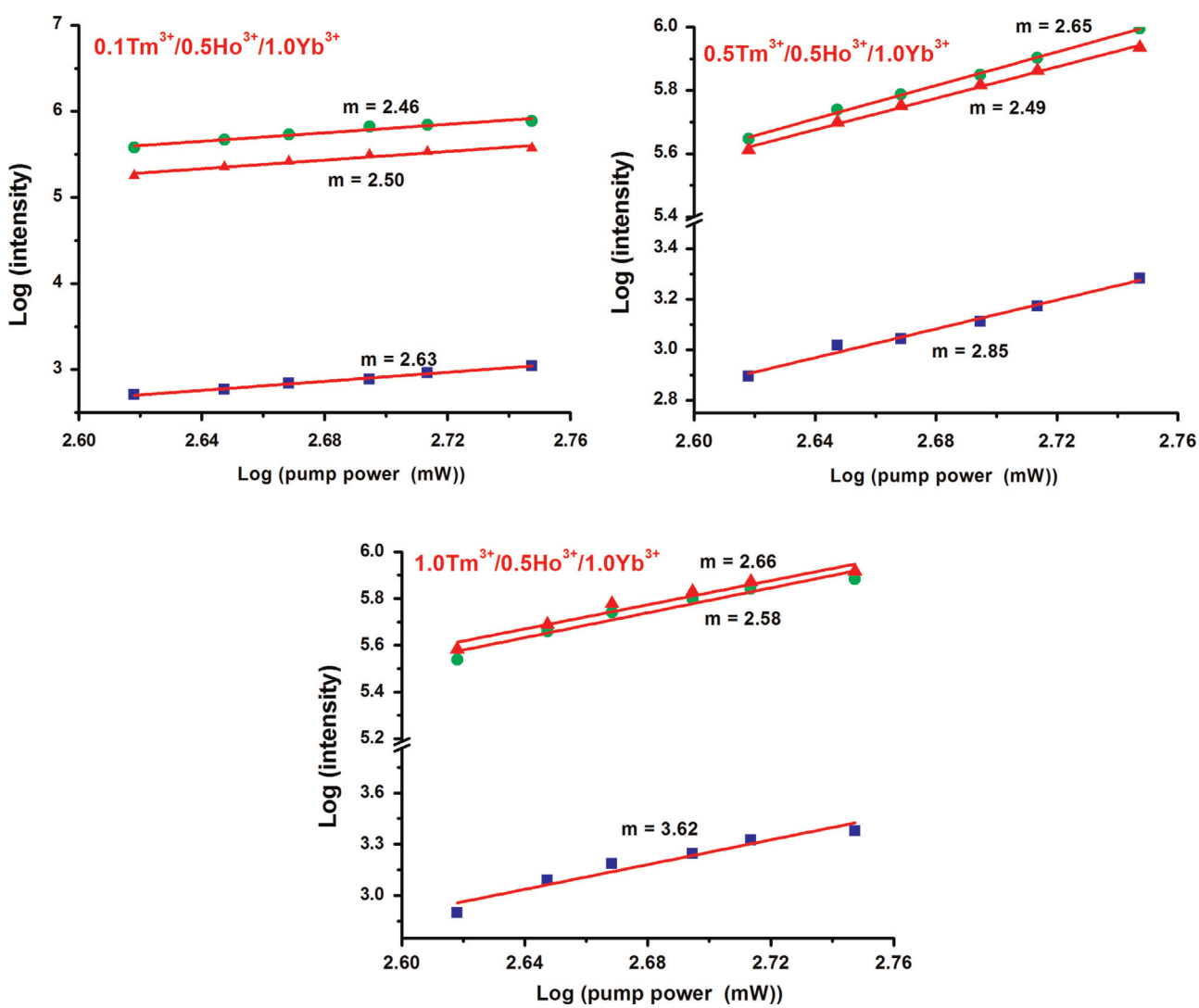

Fig. 10. Logarithmic pump power vs intensity of blue, green and red emissions in $Tm^{3+}/Ho^{3+}/Yb^{3+}$ triply doped TBZLN glasses.

3.3.2. Green and red emissions in Ho^{3+}/Yb^{3+} co-doped TBZLN glass

Up-conversion luminescence spectra of Ho^{3+}/Yb^{3+} co-doped TBZLN glass as a function of pump power laser is shown in Fig. 8. Three up-conversion luminescence bands at 546, 660 and 753 nm which could be attributed to ($^5F_4$, $^5S_2$)→$^5I_8$, $^5F_5$→$^5I_8$ and $^5F_4$($^5S_2$)→$^5I_7$ transitions of Ho^{3+} ions are observed. The intensity of primary colors at 546 (green) and 660 nm (red) as a function of pump power is also depicted in the inset of Fig. 8. It is clearly observed that emission bands at 545 nm and 660 nm present a quadratic dependence on the pumping laser power with slope values of 1.81 and 1.85, respectively, indicating that two photons contributed to each of the up-conversion emissions. It is well known that the energy transfer from Yb^{3+}→Ho^{3+} is quite effective due to proper energy matching and favourable energy levels, $^5I_6$, $^5I_7$, $^5F_5$ and $^5S_2$ metastable states of Ho^{3+} ions.

For the green and red emissions, from the schematic energy level diagram (Fig. 6), the population of $^5I_6$ level by the first energy transfer (ET1) and then Ho^{3+} at $^5I_6$ level excites to $^5F_4$ ($^5S_2$) level through the second energy transfer (ET2)

ET 1: $^2F_{5/2}$ (Yb^{3+})+$^5I_8$(Ho^{3+})→$^2F_{7/2}$(Yb^{3+})+$^5I_6$(Ho^{3+})

ET 2: $^2F_{5/2}$(Yb^{3+})+$^5I_6$(Ho^{3+})→$^2F_{7/2}$(Yb^{3+}) +$^5F_4$($^5S_2$)(Ho^{3+})

Further, the excited Ho^{3+} ions at the $^5F_4$ ($^5S_2$) level relax radiatively emitting green light at 544 nm due to $^5F_4$($^5S_2$)→$^5I_8$ transition. The red emission at 660 nm ($^5F_5$→$^5I_8$) is accomplished by populating $^5F_5$ level via the non-radiative relaxation from the $^5F_4$ ($^5S_2$) excited state and the ESA from the $^5I_7$ level.

3.3.3. . Blue, green and red emissions in $Tm^{3+}/Ho^{3+}/Yb^{3+}$ triply doped TBZLN glasses

It is well known that the combination of blue, green and red colors produce useful color range. Moreover, intense blue emission plays an important role in low and high pump power. Blue, green and red emissions with the possible energy transfer mechanisms for the Tm^{3+}/Yb^{3+} and Ho^{3+}/Yb^{3+} co-doped TBZLN glasses have been described in the previous section. Also, we made an attempt to observe the variation of blue, green and red emission intensities with the variation of Tm^{3+} ion concentration in the $Tm^{3+}/Ho^{3+}/Yb^{3+}$ triply doped TBZLN glass, and with the pump power variation. In the case of triply doped TBZLN glasses, the Yb^{3+} ions absorb efficiently the 980 nm radiation and transfer the excited energies to both Tm^{3+} and Ho^{3+} ions through the successive energy transfer process (see Fig. 6). Fig. 9 shows the blue, green and red emissions with different pump powers for the $1.0Tm^{3+}/0.5Ho^{3+}/1.0Yb^{3+}$ doped TBZLN glass. The other ($0.1Tm^{3+}/0.5Ho^{3+}/1.0Yb^{3+}$ and $0.5Tm^{3+}/0.5Ho^{3+}/1.0Yb^{3+}$) TBZLN glasses show similar band position with different intensities. Fig. 10 shows the logarithmic pump power as a function of logarithmic emission band intensity for the $xTm^{3+}/0.5Ho^{3+}/1.0Yb^{3+}$ (x=0.1, 0.5 and 1.0) triply doped TBZLN glasses. It is observed that the slope values for the blue up-conversion band are 2.63, 2.85 and 3.62 for x=0.1, 0.5, 1.0 and 1.5 of Tm^{3+} ions in $xTm^{3+}/0.5Ho^{3+}/1.0Yb^3$ triply doped TBZLN glasses, indicating the three photon excitation process of Tm^{3+} ions for blue up-conversion band. It is found that the increased trend of slope values for the blue emission band with the increasing concentration of Tm^{3+} ions is due to the sensitivity of blue excitation process with the pump power variation. It is also observed that red and green emission intensities are tuned along with the increased blue emission intensity while varying the Tm^{3+} ions in triply doped TBZLN glasses (see Fig. 11). The red and green emission intensities are nearly equal in $0.5Tm^{3+}/0.5Ho^{3+}/1.0Yb^{3+}$ doped tellurite glass, whereas in the case of $1.0Tm^{3+}/0.5Ho^{3+}/1.0Yb^{3+}$ doped TBZLN glasses red dominates the green emission intensity indicating that both Tm^{3+} and Ho^{3+} ions are responsible. Moreover, both $^1G_4$ (Tm^{3+}) and $^5I_7$ (Ho^{3+}) are metastable states which have sufficient time to allow the resonant cross-relaxation process, CR: $^1G_4$(Tm^{3+})+$^5I_7$(Ho^{3+})→$^3H_5$(Tm^{3+})+$^5S_2$(Ho^{3+}) which indeed is also responsible for the increased red emission intensity.

3.4. CIE chromaticity co-ordinate analysis

Using the CIE 1931 color model [46] and from the observed up-conversion luminescence spectra, color co-ordinates are calculated as follows:

$$x = \frac{X}{X+Y+Z}, \quad y = \frac{Y}{X+Y+Z}, \quad z = \frac{Z}{X+Y+Z} \tag{2}$$

where X, Y and Z are the tri-stimulus values which are determined from the spectrum power distribution $P(\lambda)$ described for each component as follows:

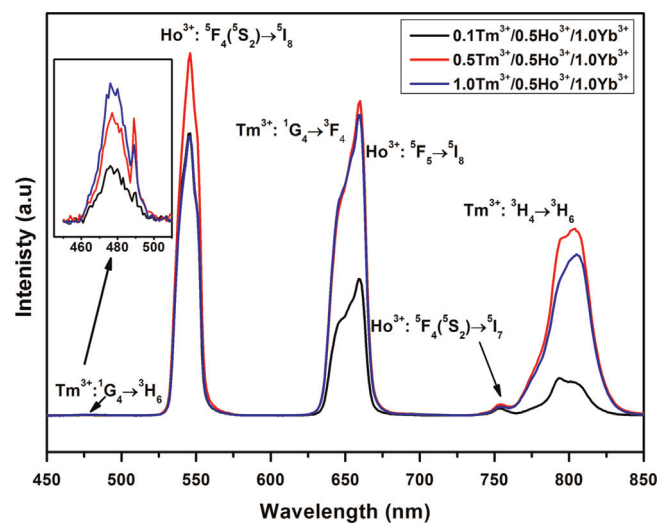

Fig. 11. Up-conversion luminescence spectra of $xTm^{3+}/0.5Ho^{3+}/1.0Yb^{3+}$ (x=0.1, 0.5 and 1.0 mol%) triply doped TBZLN glasses at 980 nm (559 mW).

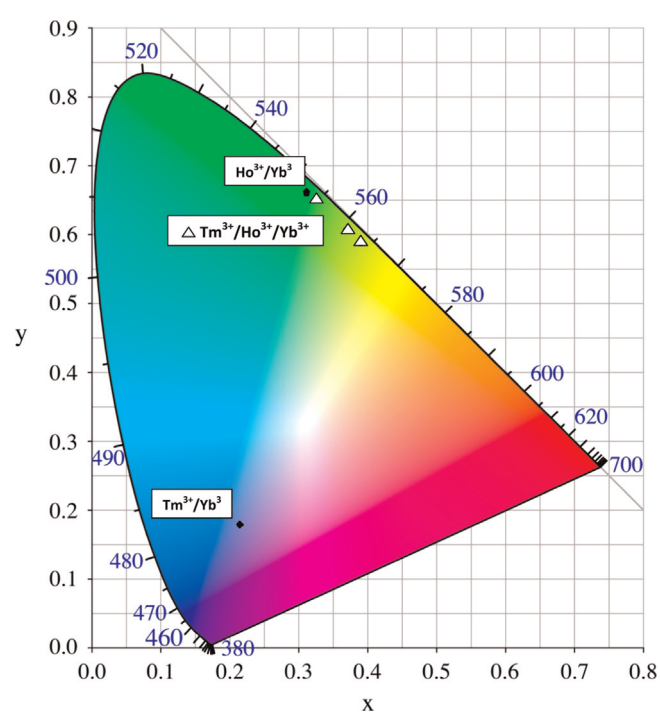

Fig. 12. CIE chromaticity diagram showing the color coordinates of Tm^{3+}/Yb^{3+}, Ho^{3+}/Yb^{3+} co-doped and $Tm^{3+}/Ho^{3+}/Yb^{3+}$ triply doped TBZLN glasses.

$$X = \int_{380}^{780} P(\lambda)\bar{x}(\lambda)\mathrm{d}\lambda,$$
$$Y = \int_{380}^{780} P(\lambda)\bar{y}(\lambda)\mathrm{d}\lambda, \quad Z = \int_{380}^{780} P(\lambda)\bar{z}(\lambda)\mathrm{d}\lambda \tag{3}$$

where λ corresponds to the monochromatic color of light wavelength, $\bar{x}$, $\bar{y}$ and $\bar{z}$ are color matching functions. The obtained co-ordinates (x=0.210, y=0.184) and (x=0.322, y=0.668) for the Tm^{3+}/Yb^{3+} and Ho^{3+}/Yb^{3+} co-doped TBZLN glasses, and (x=0.334, y=0.655), (x=0.377, y=0.613) and (x=0.397, y=0.593) for the 0.1, 0.5 and 1.0 mol%, respectively, Tm^{3+} ions in $Tm^{3+}/Ho^{3+}/Yb^{3+}$ triply doped TBZLN glasses are marked in CIE plot shown in Fig. 12. From Fig. 12, it has been noticed that the CIE co-ordinates of up-conversion spectra pertaining to Tm^{3+}/Yb^{3+} and Ho^{3+}/Yb^{3+} co-doped TBZLN glasses fall in blue and green regions of CIE diagram. As the tuning of green and red emission intensities in the $Ho^{3+}/Tm^{3+}/Yb^{3+}$ triply doped TBZLN glasses (see Fig. 11), the CIE co-ordinates moved from green region towards the greenish-yellow region due to the increase of sole blue component with Tm^{3+} concentration. This is a very important property which can be used for making various laser glasses according to the user requirement in a range of wavelengths by only varying the concentration of one of the active ions.

4. Conclusions

In summary, the oscillator strengths, radiative transition probabilities, radiative lifetimes and branching ratios of certain transition pertaining to Tm^{3+} and Ho^{3+} ions in Tm^{3+}/Yb^{3+}, Ho^{3+}/Yb^{3+} co-doped TBZLN glasses have been studied based on the J–O theory using observed absorption spectra. The higher magnitude of Ω_2 parameter indicates a strong asymmetry of the electric field around the RE ions in TBZLN glasses. McCumber's theory has been used to calculate the stimulated emission cross-section of the Tm^{3+}:$^3F_4 \rightarrow {}^3H_6$ (1.25×10^{-20} cm^2) and Ho^{3+}:$^5I_7 \rightarrow {}^5I_8$ (0.93×10^{-20} cm^2) transitions in Tm^{3+}/Yb^{3+} co-doped TBZLN glasses and are comparatively higher than the other reported glasses. The gain cross-sections for the Tm^{3+}:$^3F_4 \rightarrow {}^3H_6$ and Ho^{3+}:$^5I_7 \rightarrow {}^5I_8$ transitions are depicted from the known absorption and emission cross-section of these transitions. The visible luminescence and decay lifetimes in visible region were measured and analyzed for the Tm^{3+}, Ho^{3+} ions in $Tm^{3+}/Yb^{3+}$and Ho^{3+}/Yb^{3+} co-doped TBZLN glasses. With 980 nm laser excitation, infrared to visible luminescence was observed in all TBZLN glasses and relevant energy transfer mechanism has been discussed followed by the energy level diagram. In addition, for all TBZLN glasses, color co-ordinates were calculated from the up-conversion luminescence spectra based on CIE-1931 standards.

Acknowledgments

This work is financially supported by FAPESP, Grant # 12/50480-6. The authors would like to thank the Group of ultrafast phenomena and Optical Communications (GFURCO) and the Laboratory of Advanced Optical Spectroscopy (LMEOA//FAPESP Grant # 2009/54066-7) for providing lab facilities.

References

[1] D.C. Hanna, R.M. Percival, R.G. Smart, A.C. Tropper, Opt. Commun. 75 (1990) 283.
[2] S.Q. Xu, Z.M. Yang, J.J. Zhang, G.N. Wang, S.X. Dai, L.L. Hu, Z.H. Jiang, Chem. Phys. Lett. 385 (2004) 263.
[3] N. Rakov, G.S. Maciel, M.L. Sundheimer, L.S. Menezes, A.S.L. Gomes, J. Appl. Phys. 92 (2002) 6337.
[4] G. Galzerano, E. Sani, A. Toncelli, G.D. Valle, S. Taccheo, M. Tonelli, P. Laporta, Opt. Lett. 29 (2004) 715.
[5] D. Creeden, P.A. Ketteridge, P.A. Budni, S.D. Setzler, Y.E. Young, J.C. McCarthy, K. Zawilski, P.G. Schunemann, T.M. Pollak, E.P. Chicklis, M. Jiang, Opt. Lett. 33 (2008) 315.
[6] R. Balda, L.M. Lacha, J. Fernández, M.A. Arriandiag, J.M. Fernández- Navarro, D. Munoz-Martin, Opt. Express 16 (2008) 11836.
[7] S. Tanaba, S. Yoshii, K. Hirao, N. Soga, Phys. Rev. B 45 (1992) 4620.
[8] J. Wang, E. Vogel, E. Snitzer, Opt. Mater. 3 (1994) 187.
[9] A. Jha, S. Shen, M. Naftaly, Phys. Rev. B 62 (2000) 6215.
[10] N.K. Giri, D.K. Rai, S.B. Rai, J. Appl. Phys. 104 (2008) 113107.
[11] Y. Ledemi, D. Manzani, S.J.L. Ribeiro, Y. Messaddeq, Opt. Mater. 33 (2011) 1916.
[12] N.Q. Wang, X. Zhao, C.M. Li, E.Y.B. Pun, H. Lin, J. Lumin. 130 (2010) 1044.
[13] Y. Dwivedi, A. Rai, S.B. Rai, J. Appl. Phys. 104 (2008) 043509.
[14] H. Desirena, E. De la Rosa, P. Salas, O. Meza, J. Phys. D: Appl. Phys. 44 (2011) 455308.
[15] B.D. McSwain, N.F. Borrelli, G.J. Su, Phys. Chem. Glasses 4 (1963) 11.
[16] M. Seshadri, E.F. Chillcce, J.D. Marconi, F.A. Sigoli, Y.C. Ratnakaram, L. C. Barbosa, J. Non-Cryst. Solids 402 (2014) 141.
[17] M. Seshadri, M. Radha, D. Rajesh, L.C. Barbosa, C.M.B. Cardeiro, Y. C. Ratnakaram, Phys. B: Conden. Matter 459 (2015) 79.
[18] K. Damak, R. Maalej, E.S. Yousef, A.H. Qusti, C. Russel, J. Non-Cryst. Solids 358 (2012) 2974.
[19] M.S. Sahar, N. Noordin, J. Non-Cryst. Solids 184 (1995) 137.
[20] M. Seshadri, L.C. Barbosa, M. Radha, J. Non-Cryst. Solids 406 (2014) 62.
[21] Y.C. Ratnakaram, D. Thirupathi Naidu, A. Vijaya Kumar, J.L. Rao, J. Phys. Chem. Solids 64 (2003) 2487.
[22] S. Balaji, K. Biswas, A.D. Sontakke, G. Gupta, K. Annapurna, J. Quant. Spectrosc. Radiat. Transf. 147 (2014) 112.
[23] L. Feng, J. Wang, Q. Tang, L. Lianga, H. Lianga, Q. Su, J. Lumin. 124 (2007) 187.
[24] Y.N. Ch, Ravi Babu, P. Sree Ramnaik, A. Suresh Kumar, J. Lumin. 143 (2013) 510.
[25] B.R. Judd, Phys. Rev. 127 (1962) 750.
[26] G.S. Ofelt, J. Chem. Phys. 37 (1962) 511.
[27] K. Brahmachary, D. Rajesh, S. Babu, Y.C. Ratnakaram, J. Mol. Spectrosc. 1064 (2014) 6.
[28] S. Bose, R. Debnath, J. Lumin. 155 (2014) 210.
[29] B. Zhou, H. Lin, E.Y.B. Pun, Opt. Express 18 (2010) 18805.
[30] G. Zhao, Y. Tian, X. Wang, H. Fan, L. Hu, J. Lumin. 134 (2013) 837.
[31] R. Praveena, Kyoung Hyuk Jang, C.K. Jayasankar, Hyo Jin Seo, J. Alloy. Compd. 496 (2010) 335.
[32] B. Richards, A. Jha, Y. Tsang, D. Binks, J. Lousteau, F. Fusari, A. Lagatsky, C. Brown, W. Sibbett, Laser Phys. Lett. 7 (2010) 177.
[33] G. Gao, G. Wang, C. Yu, J. Zhang, L. Hu, J. Lumin. 129 (2009) 1042.
[34] B. Zhou, L. Tao, C.Y.Y. Chan, W. Jin, Y.H. Tsang, E.Y.B. Pun, J. Lumin. 137 (2013) 132.
[35] H. Chen, F. Chen, T. Wei, Q. Liu, R. Shen, Y. Tian, Opt. Commun. 321 (2014) 183.
[36] G. Vijaya Prakash, Mater. Lett. 46 (2000) 15.
[37] C.B. Layne, W.H. Lowdermilk, M. Weber, Phy. Rev. B 16 (1) (1977) 10.
[38] Ch Srinivasa Rao, K. Upendra Kumar, P. Babu, C.K. Jayasankar, Opt. Mater. 35 (2012) 102.
[39] M.R. Reddy, S.B. Raju, N. Veeraiah, J. Phys. Chem. Solids 61 (2000) 1567.
[40] M. Li, G. Bai, Y. Guo, L. Hu, J. Zhang, J. Lumin. 132 (2012) 1830.
[41] L. Qiongfei, X. Haiping, Z. Yuepin, W. Jinhao, Z. Jianli, H. Sailong, J. Rare Earths 27 (2009) 76.
[42] H. Fan, G. Gao, G. Wang, J. Hu, L. Hu, Opt. Mater. 32 (2010) 627.
[43] K. Biswas, A.D. Sontakke, R. Sen, K. Annapurna, Spectrochim. Acta Part A 112 (2013) 301.
[44] M. Li, Y. Guo, G. Bai, Y. Tian, L. Hu, J. Zhang, J. Quant. Spectrosc. Radiat. Transf. 127 (2013) 70.
[45] K. Pavani, L. Rama Moorthy, J. Suresh Kumar, A. Mohan Babu, J. Lumin. 136 (2013) 383.
[46] CIE colorimetry, International Commission on Illumination.